# Efficient termination of vacuolar Rab GTPase signaling requires coordinated action by a GAP and a protein kinase

Christopher L. Brett,[1] Rachael L. Plemel,[1] Braden T. Lobingier,[1] Marissa Vignali,[2] Stanley Fields,[2,3] and Alexey J. Merz [1]

[1]Department of Biochemistry, [2]Department of Genome Sciences, and [3]Howard Hughes Medical Institute, University of Washington, Seattle, WA 98195

Rab guanosine triphosphatases (GTPases) are pivotal regulators of membrane identity and dynamics, but the in vivo pathways that control Rab signaling are poorly defined. Here, we show that the GTPase-activating protein Gyp7 inactivates the yeast vacuole Rab Ypt7 in vivo. To efficiently terminate Ypt7 signaling, Gyp7 requires downstream assistance from an inhibitory casein kinase I, Yck3. Yck3 mediates phosphorylation of at least two Ypt7 signaling targets: a tether, the Vps-C/homotypic fusion and vacuole protein sorting (HOPS) subunit Vps41, and a SNARE, Vam3. Phosphorylation of both substrates is opposed by Ypt7-guanosine triphosphate (GTP). We further demonstrate that Ypt7 binds not one but two Vps-C/HOPS subunits: Vps39, a putative Ypt7 nucleotide exchange factor, and Vps41. Gyp7-stimulated GTP hydrolysis on Ypt7 therefore appears to trigger both passive termination of Ypt7 signaling and active kinase-mediated inhibition of Ypt7's downstream targets. We propose that signal propagation through the Ypt7 pathway is controlled by integrated feedback and feed-forward loops. In this model, Yck3 enforces a requirement for the activated Rab in docking and fusion.

## Introduction

Ypt/Rab proteins are small GTP-binding proteins that localize to distinct membrane domains where they coordinate vesicle motility, cargo sorting, and SNARE-mediated fusion (Segev, 2001; Zerial and McBride, 2001; Pfeffer and Aivazian, 2004; Grosshans et al., 2006). Rabs function by cycling between inactive GDP-bound and active GTP-bound states (Milburn et al., 1990). Rabs are activated by guanine nucleotide exchange factors (GEFs) that eject GDP to promote GTP binding and are inactivated by GTPase-activating proteins (GAPs) that stimulate hydrolysis of the bound GTP (Moya et al., 1993; Strom et al., 1993; Pan et al., 2006; Bos et al., 2007). The Rab-GAP superfamily shares a Tre-2/Bub2/Cdc16 (TBC) domain sufficient for substrate specificity and catalytic activity (Albert et al., 1999; Pan et al., 2006; Bos et al., 2007). Nevertheless, only a few Rab GAPs are known to operate on specific Rabs in vivo (as opposed to in vitro), and almost nothing is known about what happens to targets downstream when Rabs are inactivated by their cognate GAPs.

Important insights into the role of Rabs in membrane fusion have been obtained from cell-free assays of *Saccharomyces cerevisiae* homotypic vacuole fusion (Wickner and Haas, 2000). The vacuole is the terminal endocytic compartment equivalent to the metazoan lysosome. Vacuole fusion in vitro entails four operationally defined subreactions: priming, tethering, docking, and fusion. Priming involves ATP hydrolysis by Sec18 to activate SNAREs for docking and fusion (Sollner et al., 1993; Mayer et al., 1996; Ungermann et al., 1998). Tethering is defined by formation of adhesive contacts between the participating membranes and is promoted by the vacuolar Rab GTPase Ypt7 (Haas et al., 1995; Wang et al., 2003). Docking entails a complex set of subreactions that occur between tethering and fusion. These subreactions require active Ypt7-GTP and its Vps-C/HOPS effector complex (Rieder and Emr, 1997; Wurmser et al., 2000; Wang et al., 2002, 2003; Collins et al., 2005). Docking culminates with

Correspondence to Alex Merz: merza@u.washington.edu

Abbreviations used in this paper: CIP, calf intestinal phosphatase; GAP, GTPase-activating protein; GEF, guanine nucleotide exchange factor; HOPS, homotypic fusion and vacuole protein sorting; rGdi1, recombinant GDI1; SC, synthetic complete; TBC, Tre-2/Bub2/Cdc16.

The online version of this article contains supplemental material.



The Rockefeller University Press $30.00
J. Cell Biol. Vol. 182 No. 6 1141–1151
www.jcb.org/cgi/doi/10.1083/jcb.200801001

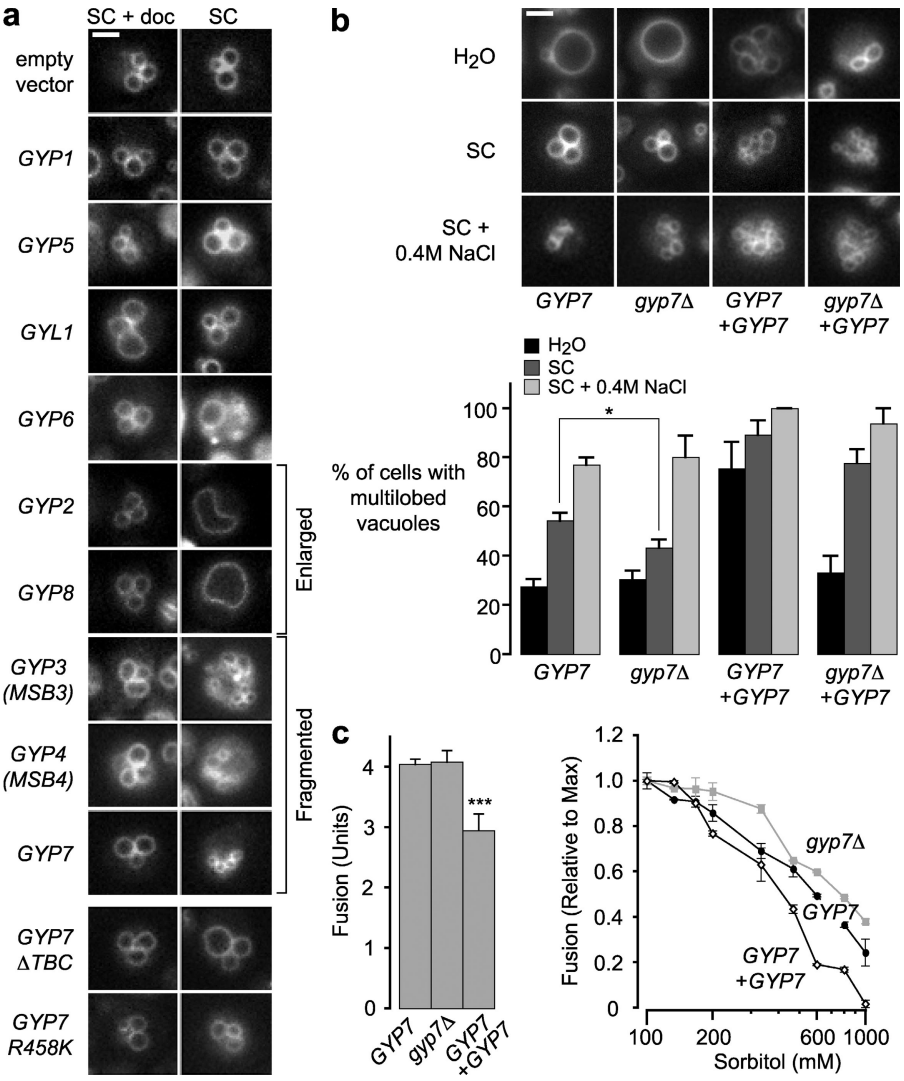


Figure 1. **Gyp7 regulates vacuole morphology in vivo and in vitro.** (a) BY4742 wild-type *S. cerevisiae*–harboring plasmids expressing each of eight *GYP* paralogues, one *GYP*-like gene (Gyl1), or two catalytically inactive Gyp7 mutants (*GYP7-ΔTBC* or *GYP7-R458K*) behind a tetracycline-repressible promotor was grown in SC medium with (repressed) or without (expressed) 5 μM doxycycline. The cells were stained with the endocytic tracer FM4-64 as described in Materials and methods, and imaged. (b) BY4742 wild-type (*GYP7*) and *gyp7*Δ cells with or without a 2-μ plasmid overexpressing *GYP7* (+*GYP7*) were stained with FM4-64, exposed to hypotonic (water), isotonic (SC), or hypertonic (SC + 0.4 M NaCl) media for either 5 min (hypotonic) or 30 min (isotonic and hypertonic). Vacuole morphology was scored as either round or multilobed according to LaGrassa and Ungermann (2005). 2,325 cells were analyzed. (c) Vacuoles isolated from BJ3505 and DKY2168 wild-type, *gyp7*Δ-, or *GYP7*-overexpressing yeast cells were incubated for 90 min in the presence of ATP and increasing concentrations of sorbitol, and homotypic vacuole fusion was measured. Similar results for *gyp7*Δ vacuoles were reported previously (Brett and Merz, 2008). $n \geq 4$ for all experiments shown. Error bars indicate mean ± SEM. Statistical significance is denoted by asterisks. *, $P \leq 0.05$; ***, $P \leq 0.001$. Bars, 2 μm.

formation of a trans-SNARE complex, an essential event that probably energizes membrane fusion (Hanson et al., 1997; Nichols et al., 1997; Weber et al., 1998; Jahn et al., 2003).

Assays of purified proteins reveal that the Rab GAP Gyp7 exhibits an in vitro preference for the vacuolar Rab Ypt7 (Wichmann et al., 1992; Vollmer et al., 1999). Purified Gyp7, its TBC domain, or the TBC domain of another GAP, Gyp1, inhibit in vitro homotypic vacuole fusion by arresting docking (Eitzen et al., 2000; Wang et al., 2003). However, it is unclear whether Gyp1, Gyp7, or other GAPs influence Ypt7 function in vivo (Zhang et al., 2005). We now show that Gyp7 targets Ypt7 in vivo but that Gyp7 cannot efficiently terminate Ypt7 signaling without downstream assistance from Yck3, the vacuolar casein kinase I. Moreover, we find that activated Ypt7 opposes Yck3-dependent phosphorylation of at least two Ypt7 signaling targets. We also show that one of these targets, the Vps-C/HOPS subunit Vps41, interacts directly with Ypt7 and that this interaction is essential for the stable association of the HOPS-tethering complex with Ypt7. Together with previous experiments, our results delineate a signaling pathway that renders the membrane fusion machinery highly responsive to the activation state of an upstream Rab GTPase.

## Results

### Endogenous Gyp7 regulates vacuole fusion in vivo and in vitro

Extensive in vitro characterization of the eight *S. cerevisiae* Rab GAPs has revealed biochemical preferences for specific Rab substrates (Table S1, available at http://www.jcb.org/cgi/content/full/jcb.200801001/DC1), but the in vivo functions of these GAPs are largely undefined. Yeast cells are viable when *GYP* genes are deleted individually, and only a fraction of the knockout mutants exhibit detectable vesicle-trafficking defects, probably because of functional redundancy (Bos et al., 2007). As an alternative approach, we overproduced each of nine Gyp or Gyp-like proteins in cells. We then performed pulse-chase labeling with the styryl dye FM4-64 to examine vacuole morphology, a common indicator of endocytic trafficking defects (Fig. 1 a). Overproduction of Gyp1, Gyp5, or Gyl1 did not cause overt changes in vacuole morphology. Overproduction of Gyp2 and Gyp8 caused enlargement of the vacuole. In vitro, Gyp2 and Gyp8 stimulate GTP hydrolysis on Ypt6, which controls endosomal retrograde traffic, and on Sec4, which controls exocytosis of secretory vesicles. Thus, Gyp2 and Gyp8 may coordinate the

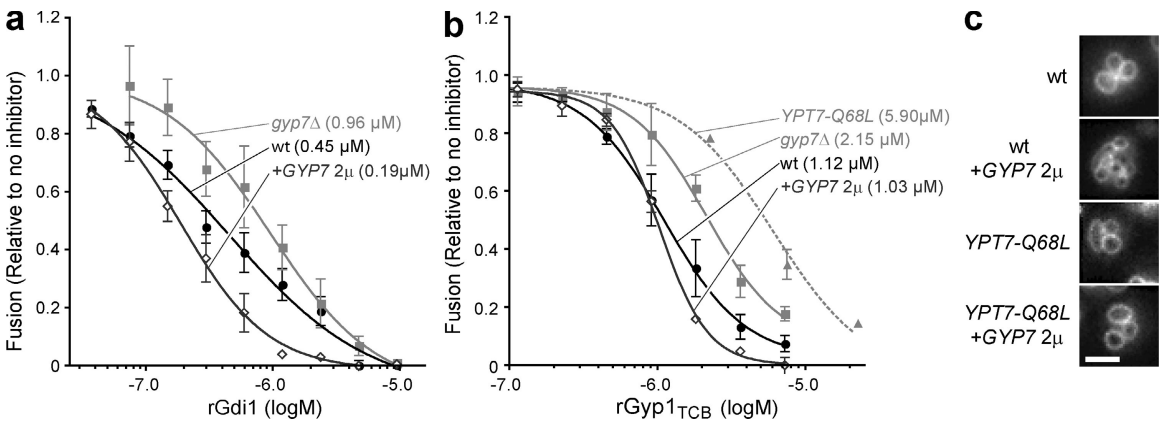


Figure 2. **Gyp7 prevents vacuole fusion by inactivating Ypt7.** (a and b) Homotypic fusion was measured with vacuoles isolated from BJ3505 and DKY2168 wild-type (wt), *gyp7*Δ, $YPT7_{Q68L}$, or *GYP7*-overexpressing cells (+*GYP7* 2μ). Vacuoles were incubated with ATP for 90 min in the presence of increasing concentrations of rGdi1 (a) or $rGyp1_{TBC}$ (b). The mean fusion values were fit to sigmoidal dose–response curves ($r^2 > 0.98$). $IC_{50}$ values for the fits are shown in parentheses. $n \geq 4$ for all experiments shown. Error bars indicate mean ± SEM. (c) Wild-type DKY6128 cells containing chromosomal copies of wild-type *YPT7* or the GTP hydrolysis-deficient allele $YPT7_{Q68L}$ in the presence or absence of *GYP7* expressed from a high copy 2-μm plasmid were grown in SC medium, stained with FM4-64, and imaged. Bar, 2 μm.

inhibition of multiple Rabs within the cell to oppose secretion and retrograde endosomal traffic, shunting membrane to the vacuole. Gyp6, like Gyp2 and Gyp8, has an in vitro preference for Ypt6, but, unlike Gyp2 and Gyp8, it does not stimulate GTP hydrolysis on Sec4. Overproduction of Gyp6 caused accumulation of additional endosomal structures (Fig. 1 a), suggesting that Gyp6 more selectively opposes endosomal retrograde transport or endosome–vacuole fusion, as suggested by previous experiments (Ali et al., 2004). Overproduction of three Gyps, Gyp3/Msb3, Gyp4/Msb4, and Gyp7, caused vacuoles to fragment, consistent with reduced vacuole fusion. Gyp3 and Gyp4 are implicated in polarized exocytosis and appear to be functionally redundant, although they have divergent in vitro Rab specificities (Table S1; Gao et al., 2003). In vitro, both Gyp1 and Gyp7 inactivate Ypt7 and inhibit homotypic vacuole fusion (Eitzen et al., 2000). However, Gyp7 overexpression in vivo caused vacuoles to fragment, whereas Gyp1 overexpression did not (Fig. 1 a). Thus, the in vitro selectivity of a Rab GAP is often, but not always, a reliable indicator of its in vivo functions. Our data suggest that Gyp7, and possibly Gyp3 and Gyp4, are bona fide negative regulators of Ypt7.

In separate experiments, we uncovered a role for Gyp7 in vacuole fusion when hyperosmotic stress was applied to purified vacuoles in vitro (Brett and Merz, 2008). Upon exposure of wild-type cells to hypotonic conditions, vacuoles fuse within seconds (Bone et al., 1998; Wang et al., 1998, 2002), whereas upon exposure to hypertonic medium, vacuoles fragment within minutes (Bone et al., 1998; LaGrassa and Ungermann, 2005). We therefore assessed the in vivo consequences of *GYP7* overexpression or deletion on vacuole morphology in cells grown under various osmotic conditions (Fig. 1 b). The *gyp7*Δ deletion allele decreased fragmentation slightly but significantly under standard conditions (Fig. 1 b), whereas overexpression of *GYP7* from a high copy plasmid resulted in severely fragmented or multilobed vacuoles under all conditions, consistent with the idea that Gyp7 negatively regulates vacuole fusion in vivo (Fig. 1 b). Overexpression of *GYP7* in *gyp7*Δ mutant cells also increased vacuole fragmentation compared with wild-type cells. This fragmentation required Gyp7 with an intact catalytic TBC domain. Overexpression of Gyp7 lacking the TBC domain or with a mutated catalytic arginyl residue within the TBC domain (R458K) was without effect (Fig. 1 a, bottom). These results support the hypothesis that Gyp7 opposes Ypt7 action in vivo.

To further evaluate the role of Gyp7, we assayed the in vitro homotypic fusion of vacuoles isolated from *gyp7*Δ mutant and *GYP7* overexpressor cells (Fig. 1 c). In the standard assay of homotypic fusion, vacuoles are isolated from two yeast strains by equilibrium floatation: vacuoles from *pep4*Δ *PHO8* cells contain inactive alkaline phosphatase, proPho8, whereas vacuoles from *PEP4 pho8*Δ cells lack proPho8 but contain a maturase needed for Pho8 activation. Membrane fusion between the two types of vacuoles results in lumenal content mixing and Pho8 activation, which is then quantified with a colorimetric assay to obtain an index of fusion (Wickner and Haas, 2000; Merz and Wickner, 2004a). Ypt7 inactivation occurs when vacuoles are exposed to hypertonic stress (Brett and Merz, 2008). Vacuoles isolated from *gyp7*Δ cells were reduced in sensitivity to hypertonic stress; conversely, vacuoles isolated from *GYP7* overexpressors exhibited enhanced sensitivity to hypertonic stress (Fig. 1 c). Together, our results indicate that Gyp7 opposes Ypt7-dependent homotypic vacuole fusion both in vivo and in vitro.

### Gyp7 inactivates Ypt7p in vivo

If Gyp7 modulates Ypt7 activity in vivo, we would expect that vacuoles isolated from *gyp7Δ* mutant or *GYP7* overexpressor cells should bear different amounts of active Ypt7, and fusion of these vacuoles should exhibit modified sensitivity to Ypt7 inhibitors. To test these predictions, we performed dose-inhibition studies (Fig. 2 a) with recombinant GDI1 (rGdi1), a Rab chaperone that inhibits fusion by preferentially extracting inactive Rab–GDP complexes from membranes. As predicted, vacuoles isolated from *gyp7*Δ cells were less sensitive to rGdi1 than vacuoles from wild-type cells, whereas vacuoles isolated from *GYP7* overexpressors were more sensitive to rGdi1 (Fig. 2 a).

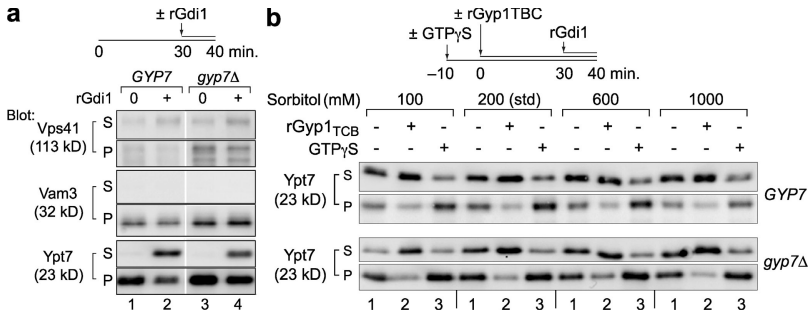


Figure 3. **Native Gyp7 inactivates Ypt7p in vivo.** (a) Vacuoles isolated from BJ3505 wild type (*GYP7*) or *gyp7*Δ were incubated with ATP for 40 min with 9.5 µM rGdi1 absent or present during the last 10 min. Vacuoles were sedimented, and membrane association of Vps41, Vam3, and Ypt7 was assessed by immunoblotting. The white line indicates that intervening lanes have been spliced out. (b) Vacuoles isolated from BJ3505 wild-type (*GYP7*, top) or *gyp7*Δ cells (bottom) were pretreated with or without 200 µM GTPγS for 10 min at 27°C and incubated for 40 min with ATP in the presence or absence of 3.6 µM $rGyp1_{TBC}$ at four concentrations of sorbitol (standard conditions). During the last 10 min of incubation, 9.5 µM rGdi1 was added. Vacuoles were immediately sedimented, and the membrane distribution of Ypt7 was assessed by immunoblotting. One third of the total isolated supernatant (S) and one fifth of the pellet (P) were analyzed by immunoblotting.

Similarly, vacuoles lacking Gyp7 were reduced in sensitivity to the recombinant catalytic domain of Rab-GAP Gyp1 ($rGyp1_{TBC}$). In contrast, removal of endogenous Gyp7 did not alter dosage sensitivity to three inhibitors of fusion that do not target Ypt7: anti-Sec17 antibody, which blocks the early priming stage; anti-Vam3 antibody, which blocks SNARE function during docking; and MARCKS effector domain peptide, a late-stage inhibitor that chelates acidic lipid headgroups (Wang et al., 2003; Thorngren et al., 2004). To verify that $rGyp1_{TBC}$ inhibits fusion by inhibiting Ypt7 and not some other target (e.g., another Rab) on the vacuole, we used a GTP-"locked" Ypt7 mutant, $Ypt7_{Q68L}$, which exhibits an 85% reduction in both intrinsic and GAP-stimulated GTP hydrolysis in vitro (Albert et al., 1999; Vollmer et al., 1999; Pan et al., 2006). In agreement with this result, in vitro fusion of vacuoles bearing $Ypt7_{Q68L}$ was 80% less sensitive to $rGyp1_{TBC}$ compared with vacuoles from wild-type cells (Fig. 2 b). Similarly, we found that the in vivo vacuole fragmentation caused by Gyp7 overproduction was suppressed by the $YPT7_{Q68L}$ allele (Fig. 2 c). Collectively, these results demonstrate that endogenous Gyp7 decreases the amount of functionally active Ypt7 on the vacuole.

To obtain a biochemical readout of the activation state of vacuolar Ypt7, we isolated vacuoles from *gyp7*Δ mutant cells or isogenic wild-type cells, incubated the vacuoles under fusion conditions, and briefly exposed them to rGdi1. Centrifugation was used to separate soluble from membrane pellet fractions (Fig. 3 a). Slightly more Ypt7 copurified with vacuoles from *gyp7*Δ cells compared with wild-type cells (Fig. 3 a, compare lane 1 with lane 3). Importantly, although rGdi1 extracted a majority of the Ypt7 on vacuoles isolated from wild-type cells, it extracted less than half of the Ypt7 on vacuoles from *gyp7*Δ cells (Fig. 3 a, compare lane 2 with lane 4; and Fig. 3 b, lane 1, 200-mM sorbitol condition). This result indicates that on vacuoles lacking Gyp7, an increased fraction of Ypt7 is in the active GTP-bound state. In addition, we examined the Ypt7 effector complex Vps-C/HOPS, which requires Ypt7 for its stable retention on the vacuole (Eitzen et al., 2000; Price et al., 2000; Seals et al., 2000). Like Ypt7, the HOPS subunit Vps41 was enriched on vacuoles isolated from *gyp7*Δ cells (Fig. 3 a), and a reduced fraction of Vps41 was released into the supernatant by rGdi1 treatment when Gyp7 was absent. Thus, the ratio of Ypt7:GTP to Ypt7:GDP is elevated on vacuoles obtained from *gyp7*Δ cells.

We next examined Ypt7 activity in wild-type and *gyp7*Δ cells under physical conditions that increase or decrease Ypt7-mediated tethering and docking (Fig. 3 b). We recently found that Ypt7 is stabilized on membranes when the osmotic strength of the assay buffer is reduced (Brett and Merz, 2008). A corresponding biochemical stabilization of Ypt7 was readily observed on vacuoles isolated from *gyp7*Δ versus *GYP7* cells as the sorbitol concentration was varied (Fig. 3 b, compare lanes 1). Endogenous Gyp7 therefore modulates the sensitivity of Ypt7 extraction to changes in osmotic strength.

Three observations indicate that Ypt7 stabilization on vacuoles lacking Gyp7 results from decreased GTP hydrolysis, not from increased nucleotide exchange or an intrinsic resistance of Ypt7 to Gdi1-mediated extraction. First, GTP was not normally added to our cell-free reactions (Fig. 3, a and b, lanes 1); thus, stabilization of active Ypt7 does not require nucleotide exchange. Second, addition of $rGyp1_{TBC}$ resulted in almost complete extraction of Ypt7 under all conditions, indicating that unextracted Ypt7 is not intrinsically resistant to rGdi1 (Fig. 3 b, lanes 2). Third, and most importantly, preincubation of the vacuoles with GTPγS, a poorly hydrolyzable analogue of GTP, almost completely blocked Ypt7 extraction by rGdi1 (Fig. 3 b, lanes 3), indicating that Gdi1 is, as expected, preferentially extracting inactivated Ypt7. These findings were further supported by fusion experiments with rGdi1, $rGyp1_{TBC}$, and GTPγS (Fig. S1, available at http://www.jcb.org/cgi/content/full/jcb.200801001/DC1). Collectively, the results presented in Figs. 1–3 establish Gyp7 as a major in vivo GAP of Ypt7.

## Yck3p acts at the vacuole to oppose fusion

In addition to Gyp7, vacuole fusion is opposed by the casein kinase I Yck3 (LaGrassa and Ungermann, 2005). Yck3 localizes mainly to the vacuole, but it could oppose vacuole fusion either directly or indirectly (for example, by altering membrane recycling pathways). The latter possibility was a significant concern because Vps41, the only protein so far reported to be a target of Yck3, has been proposed to have roles in membrane budding as well as fusion (Rehling et al., 1999; Price et al., 2000). Yck3 requires ATP to function as a protein kinase, so we reasoned that removal of ATP should mimic the effects of Yck3 deletion. To test this idea, we exploited our finding that the recombinant SNARE rVam7 drives on pathway Rab- and SNARE-dependent

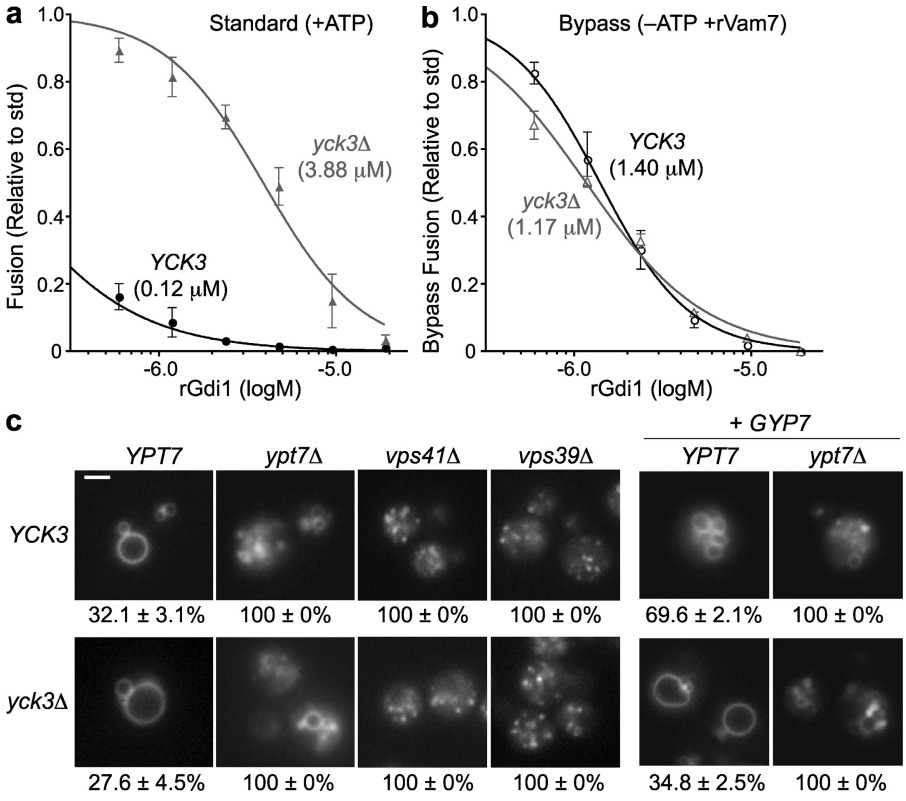


Figure 4. **Yck3 functions downstream of Ypt7 on the vacuole.** Vacuoles isolated from BY4742 *pep4*Δ and *pho8*Δ wild- type cells (*YCK3*) or *yck3*Δ cells were incubated with either ATP (a) or rVam7 (b) for 90 min in the presence of increasing concentrations of rGdi1. Fusion activity was measured and is shown as a fraction of the activity observed in the absence of rGdi1. Datasets were fit to sigmoidal dose–response curves ($r^2 > 0.97$); the $IC_{50}$ values for the fits are shown in parentheses. Error bars indicate mean ± SEM. (c) BY4742 single or double mutant cells with the indicated genotypes were grown without (left) or with (right) the *GYP7* overexpression plasmid pYADH1-*GYP7*-His6 and stained with FM4-64 under isotonic conditions. Vacuole morphology was scored, and the fraction of cells with fragmented or multilobed vacuoles is indicated for each strain. 3,836 cells were analyzed. $n \geq 4$ for all experiments shown. Bar, 3 μm.

fusion, bypassing the usual requirement for ATP and the Sec18 ATPase (Merz and Wickner, 2004b; Thorngren et al., 2004). Standard ATP-driven fusion reactions with vacuoles isolated from *yck3*Δ cells were highly resistant to rGdi1 when compared with reactions containing purified vacuoles from *YCK3* cells (Fig. 4 a), as reported previously (LaGrassa and Ungermann, 2005). In rVam7-driven ATP bypass reactions, however, there was no difference in rGdi1 sensitivity between vacuoles from *YCK3* and *yck3*Δ cells (Fig. 4 b). Comparable results were obtained using $rGyp1_{TBC}$ instead of rGdi1 (unpublished data). Together, these results show that under conditions in which vacuolar Yck3 cannot operate, vacuoles from *YCK3* and *yck3*Δ strains have indistinguishable sensitivity to Rab inhibitors. With purified vacuoles, the effect of Yck3 manifests only under conditions in which the kinase can function, indicating that Yck3 must oppose Ypt7-stimulated fusion through immediate action on the vacuole, not through an indirect effect on membrane traffic.

### *YPT7* is epistatic to *YCK3*

The mechanisms by which Ypt7 promotes fusion are unclear. The 30-fold greater resistance of in vitro fusion to Ypt7 inhibitors when Yck3 is absent raised the possibility that the main function of Ypt7-GTP is to counteract an inhibitory effect of Yck3. This model predicts that if Yck3 is removed, Ypt7 should not be needed for fusion. Conversely, if other functions of Ypt7 (such as propagating a positive signal through the Vps-C/HOPS complex) are essential, both Ypt7 and its effectors should be needed for fusion in both the presence and absence of Yck3. To test these predictions, we constructed double mutant cells lacking Yck3 and Ypt7, Vps39, or Vps41. We then examined vacuole morphology using FM4-64 dye loading (Fig. 4 c). In the absence of Ypt7, the FM4-64–labeled vacuolar compartment was fragmented in every cell examined, whether Yck3 was present or absent. We found a similar epistasis relationship in growth assays (Fig. S2, available at http://www.jcb.org/cgi/content/full/jcb.200801001/DC1). Deletion of *YCK3* also failed to suppress vacuole morphology defects in cells lacking either of two major Ypt7-binding partners, the Vps-C/HOPS subunits Vps39 (Wurmser et al., 2000) and Vps41 (see this paper). *YPT7*, *VPS39*, and *VPS41* are therefore epistatic to *YCK3*. Because the Rab and its binding partners are needed for fusion in both the presence and absence of Yck3, Yck3 appears to function as a modulator of the Ypt7 signaling pathway.

To test Yck3 function under conditions in which Ypt7 function is compromised but not eliminated, we performed an in vivo version of the in vitro experiment shown in Fig. 4 a by overexpressing *GYP7* in a *yck3*Δ mutant (Fig. 4 c). As shown in Fig. 1, *GYP7* overexpression in a wild-type cell caused vacuolar fragmentation. In sharp contrast, fragmentation did not increase when *GYP7* was overexpressed in *yck3*Δ mutant cells (Fig. 4 c). Thus, the in vivo and in vitro results are fully consistent and together reveal *YCK3* as a classical modifier. *YCK3* renders the *YPT7* pathway far more sensitive to inhibition, but removal of *YCK3* does not abrogate requirements for *YPT7*, *VPS39*, or *VPS41*.

### Ypt7 opposes Yck3-mediated phosphorylation of Vps41 and Vam3

We next sought biochemical correlates of the functional and genetic interactions among Ypt7, Vps41, Gyp7, and Yck3. It was shown previously that Vps41, a subunit of the Ypt7 effector complex Vps-C/HOPS, is phosphorylated in a reaction that requires *YCK3* (LaGrassa and Ungermann, 2005). This can be

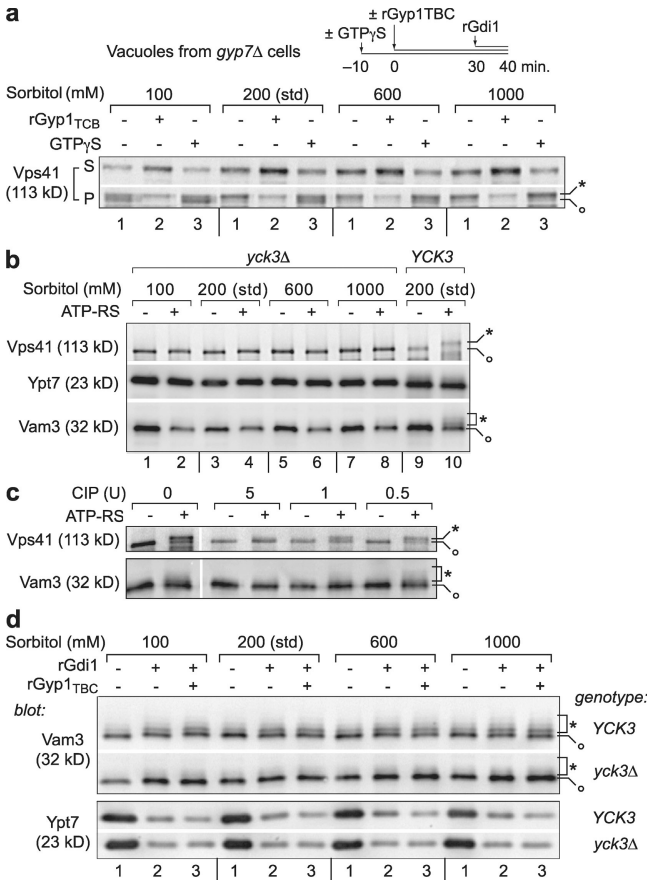


Figure 5. **Ypt7-GTP opposes Yck3-mediated phosphorylation of Ypt7 targets.** (a) Vacuoles isolated from BJ3505 *gyp7*Δ cells were subjected to the same analysis as in Fig. 3 b, and the membrane distribution of Vps41 was assessed by immunoblotting. (b) Vacuoles isolated from BY4742 *pep4*Δ wild-type (*YCK3*) or *yck3*Δ cells were incubated for 70 min with or without ATP in the presence of increasing concentrations of sorbitol. Only standard conditions (200 mM sorbitol) are shown for *YCK3* vacuoles. Vacuoles were immediately sedimented, and membrane pellets were assayed for Vps41, Vam3, and Ypt7 by immunoblotting. (c) BY4742 *pep4*Δ vacuoles were incubated for 70 min with or without ATP in the presence or absence of three concentrations of CIP. Vacuoles were sedimented, and immunoblot analysis was performed on the membrane pellets to assess Vps41 and Vam3. (d) Vacuoles isolated from BY4742 *pep4*Δ wild-type (*YCK3*) or *yck3*Δ cells were incubated for 70 min with ATP in the presence or absence of 9.5 µM rGdi1 or 3.6 µM rGyp1$_{TBC}$ at four concentrations of sorbitol. Vacuoles were sedimented, and immunoblot analysis was performed on the membrane pellets to assess Vps41 and Vam3. One fifth of the total membrane pellet was used for these analyses. Note the collapse of high $M_r$ forms (*) of Vps41 and Vam3 to the low $M_r$ form (o) when GTPγS is present, sorbitol is decreased, *YCK3* is deleted, CIP is added, or rGdi1 is absent.

assayed by immunoblotting because phospho-Vps41 migrates slowly through SDS–polyacrylamide gels. Under standard in vitro vacuole fusion conditions, Vps41 phosphorylation was rapid and quantitative. Vps41 phosphorylation was inhibited, however, under conditions that activate or stabilize Ypt7, an effect readily observed when Gyp7 was absent (Fig. 5 a). Under standard reaction conditions (Fig. 5 a, 200 mM sorbitol, lane 1), most membrane-associated Vps41 was found in a slow-migrating band (Fig. 5 a, *). However, the faster-migrating, nonphosphorylated form (Fig. 5 a, o) became more abundant when Ypt7 was further stabilized, either by preincubating the vacuoles with GTPγS (Fig. 5 a, compare 200 mM sorbitol, lanes 1 and 3) or by lowering the buffer osmotic strength (Brett and Merz, 2008; Fig. 5 a, compare 200 mM with 100 mM sorbitol, lanes 1). The strongest inhibition of phosphorylation occurred when low osmolarity (Fig. 5 a, 100 mM sorbitol) and GTPγS were combined (Fig. 5 a, compare 100 mM sorbitol, lane 3 vs. 200 mM sorbitol, lane 1). Conversely, inactivation of Ypt7 with rGyp1$_{TBC}$ enhanced Vps41 phosphorylation and dissociation from the membrane (Fig. 5 a, lanes 2). Ypt7-GTP therefore opposes Yck3-dependent phosphorylation of Vps41.

The $Q_a$-SNARE Vam3 is a core component of the vacuolar membrane fusion machinery and is essential for homotypic fusion. As with Vps41, we found that Vam3 is phosphorylated in a Yck3-dependent, Ypt7-inhibited reaction. ATP treatment resulted in slower Vam3 migration through SDS–polyacrylamide gels (Fig. 5 b, compare lane 9 with lane 10), and this observed change in Vam3 mobility is the result of phosphorylation. As previously reported for Vps41 (LaGrassa and Ungermann, 2005), slow-migrating Vam3 bands appeared only when ATP was supplied, and the slow-migrating bands for both Vps41 and Vam3 vanished upon exposure to alkaline phosphatase (Fig. 5 c). Slow-migrating, ATP-dependent phosphorylation products of both Vps41 and Vam3 appeared on vacuoles from *YCK3* cells but were absent on vacuoles from *yck3*Δ mutant cells (Fig. 5 b, compare lanes 1–8 with lanes 9 and 10; and Fig. 5 d). Moreover, Vam3 phosphorylation, like Vps41 phosphorylation, was opposed by Ypt7-GTP (Fig. 5 d), as inhibition of Ypt7 with rGdi1 in the presence or absence of rGyp1$_{TBC}$ enhanced Vam3 phosphorylation at all sorbitol concentrations tested (Fig. 5 d, compare lanes 1 with lanes 2 and 3). Thus, at least two functional targets of Ypt7 (Vps41 and Vam3) are phosphorylated in Yck3-dependent reactions that occur on the vacuole, and phosphorylation of both targets is opposed by active Ypt7-GTP.

## HOPS subunit Vps41 contains a Ypt7-binding site

The inhibition of Vps41 phosphorylation by activated Ypt7 (Fig. 5) raised the possibility that Ypt7 and Vps41 interact directly. The HOPS subunit Vps39 was reported to preferentially interact with unliganded Ypt7 and Ypt7-GDP (Wurmser et al., 2000), but in other experiments, the HOPS holocomplex was selectively captured on Ypt7-GTPγS affinity resins (Price et al., 2000; Seals et al., 2000). The divergent nucleotide specificities seen in these experiments suggested that the HOPS holocomplex might contain more than one Ypt7-binding site.

Fortuitously, a whole genome yeast two-hybrid screen for proteins that interact with the N-terminal region of Vps41 yielded only three strong hits from an ordered prey array of >5,000 yeast ORFs: Ypt7, Vam3, and Csm3 (Fig. S3 a, available at http://www.jcb.org/cgi/content/full/jcb.200801001/DC1). In retests against a miniarray of independently constructed and validated prey constructs, the Vps41–Vam3 interaction was not consistently reproduced, but Vps41 and Ypt7 interacted robustly in every experiment (Fig. 6). The Ypt7 prey interacted with bait constructs containing either full-length Vps41 or an N-terminal fragment of Vps41 (residues 99–500), but Ypt7 failed to interact with bait constructs containing the C-terminal half of Vps41 (residues 501–992). Moreover, Vps41 failed to interact with a series of

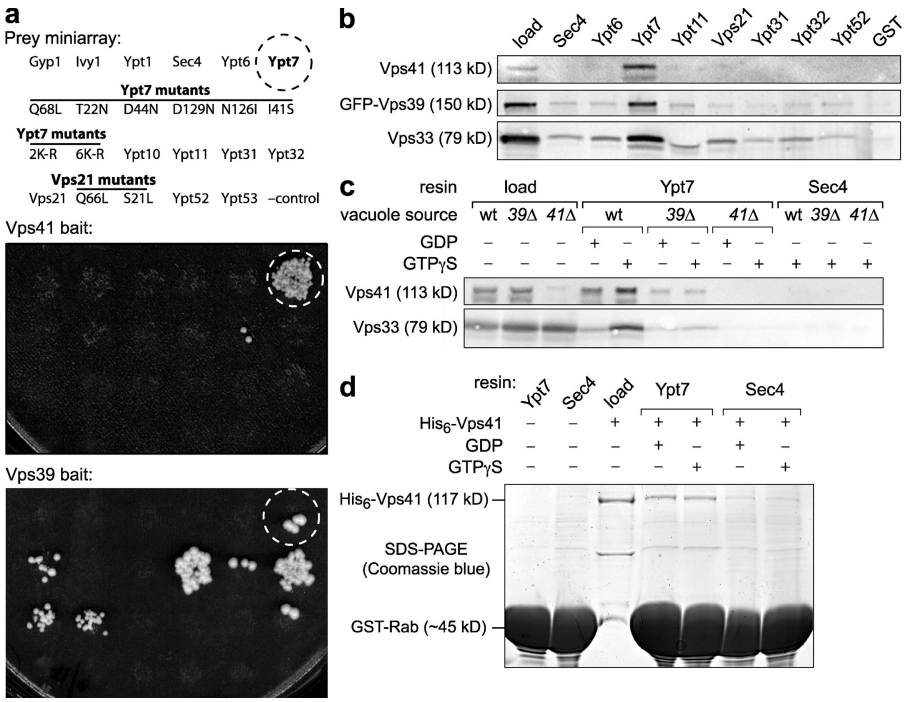


Figure 6. **A second Ypt7-binding site in Vps-C/HOPS subunit Vps41.** (a) Two-hybrid interaction tests were performed by mating cells harboring the indicated bait constructs against a miniarray of prey constructs as indicated, selecting for diploid cells, and replica plating the diploid cells to selective medium lacking histidine and containing 3-aminotriazole to increase stringency (see Materials and methods). The prey miniarray contains all 11 yeast Rab GTPases as well as mutant forms of Vps21 and Ypt7. The wild-type Ypt7 prey is indicated by a dashed circle. The Ypt7 or Vps21 mutants shown affect nucleotide binding; e.g., Ypt7-D129N and -I41S are predicted to have reduced affinity for both GDP and GTP. 2K and 6K mutants contain Arg substitutions at Lys residues reported to be ubiquitylated in native Ypt7 (Kleijnen et al., 2007). (b) Pull-down experiments were performed using eight different GST-Rab fusions or GST alone with cell lysates from BJ3505 Vps39-GFP cells. The amount of Vps41, Vps39-GFP, or Vps33 bound to the GST-Rab resin or found in lysate (load) was determined by immunoblotting. GST-Ypt11 is similar in size to Vps33, interfering with the migration of Vps33 in the Ypt11 lane. (c) Pull-down experiments were performed with either GST-Ypt7 or GST-Sec4 and lysates from BY4742 wild-type (wt), vps39Δ (*39*Δ), or *vps41*Δ (*41*Δ) cells in the presence of 200 µM GDP or GTPγS. Vps41 or Vps33 in the load and eluate fractions was detected by immunoblotting. (d) Pull-down experiments were performed with either GST-Ypt7 or GST-Sec4 resins and 200-nM recombinant full-length Vps41 (rVps41) in the presence of 200 µM GDP or GTPγS. Input and bound proteins were separated by SDS-PAGE and stained with Coomassie brilliant blue.

Ypt7 point mutants. In sharp contrast, Vps39 or N-terminal Vps39 fragments interacted with a broad spectrum of Ypt7 mutants (Fig. 6) and interacted more robustly with some mutant alleles of Ypt7 than with the wild-type construct. The preferential recognition of different Ypt7 alleles by Vps39 and Vps41 provides strong evidence that the binding sites of these proteins recognize different features or states of Ypt7.

In previous studies (Price et al., 2000; Seals et al., 2000; Wurmser et al., 2000; LaGrassa and Ungermann, 2005), Vps39 and HOPS were shown to bind Ypt7 preferentially over Vps21 and Ypt1, but binding to the other eight yeast Rab proteins has not previously been evaluated. We found that neither Vps39 nor Vps41 interacted strongly with any yeast Rab other than Ypt7, indicating a high degree of binding selectivity. In an additional control performed to verify the specificity of the prey miniarray, Vac1, a known effector of the endosomal Rab Vps21, interacted with Vps21 and an activated Vps21 allele (Fig. S3 b) but not with Ypt7 or any other yeast Rab.

To further scrutinize Ypt7–Vps41 interactions, we performed affinity pull-down experiments using yeast cell lysates and resins decorated with GST-Rab fusion proteins. Consistent with our results from two-hybrid experiments (Fig. 6 a), Vps41 was retained on GST-Ypt7–GTPγS but not on seven other GST-Rab–GTPγS affinity matrices. The other component of HOPS known to bind Ypt7 directly, Vps39, exhibited a similar selectivity for Ypt7 over other Rabs in these experiments. Vps33, a component of both the Vps-C/HOPS and Vps-C/CORVET complexes, controls traffic to the prevacuolar endosome (Peplowska et al., 2007). Vps33 bound to Ypt7 preferentially, but it also bound other Rabs to a lesser extent, including the endosomal Rab Vps21 (Fig. 6 b). Together with our yeast two-hybrid results, these results demonstrate for the first time that Vps-C/HOPS interacts quite selectively with Ypt7 but not with any other *S. cerevisiae* Rab.

We next examined the relative contributions of Vps39 and Vps41 in the binding of HOPS to Ypt7 (Fig. 6 c). This experiment is possible because *vps39*Δ and *vps41*Δ mutant cells contain stable hybrid Vps-C complexes in which Vps39 or Vps41 are replaced by Vps3 or Vps8 (Peplowska et al., 2007). As reported previously, the HOPS holocomplex preferentially bound Ypt7 in the presence of GTPγS (Fig. 6 c; Price et al., 2000; Seals et al., 2000; Peplowska et al., 2007). In the absence of Vps39, however, HOPS binding to Ypt7 declined substantially, and the apparent nucleotide selectivity was lost (Fig. 6 c). In the absence of Vps41, HOPS binding to Ypt7 was undetectable, demonstrating that Vps41 is essential for stable Ypt7-HOPS binding. To test whether Ypt7 and Vps41 interact directly, pull-down experiments were performed using purified recombinant proteins. Consistent with the two hybrid assays (Fig. 6 a) and results obtained using lysates from *vps39*Δ cells (Fig. 6 c), full-length Vps41 bound to Ypt7 but not to Sec4. The Vps-C/HOPS complex therefore contains a minimum of two distinct and highly selective Ypt7-binding sites: one site resides in the presumed GEF, Vps39, and a second site resides in the N-terminal portion of Vps41.

## Discussion

A great deal is known about the enzymology of Rab regulation, but far less is known about how Rabs are regulated in the context of cellular physiology. The present experiments delineate a pathway that enforces the tight coupling of a membrane docking and fusion machinery to the activation state of its cognate Rab GTPase (Fig. 7). First, we show that the Rab7 paralogue

Ypt7, which controls fusion at the lysosomal vacuole of budding yeast, is inactivated in vivo by a cognate GAP, Gyp7, confirming a relationship previously implied by in vitro assays with purified proteins (Vollmer et al., 1999; Eitzen et al., 2000; Pan et al., 2006). Second, we show that the casein kinase Yck3 acts directly at the vacuole as a downstream negative regulator of Ypt7 signaling. Third, we show that the Gyp7 GAP cannot efficiently terminate Ypt7 signaling in the absence of Yck3 in vivo. Fourth, we show that activated Ypt7-GTP acts to block Yck3-dependent phosphorylation of at least two of its own functional targets: the HOPS subunit Vps41 and the Vam3 SNARE. Finally, we demonstrate that Vps41 contains a Ypt7-binding site and is essential for stable HOPS binding to Ypt7.

In our working model (Fig. 7), the signaling state of Ypt7 is controlled by an activating GEF (probably Vps39; Wurmser et al., 2000) and an inhibitory GAP (Gyp7), whereas the coupling of downstream functions to Ypt7 activation is enforced by the Yck3 kinase, which inhibits Rab targets, increasing the amount of activated Rab required to generate a functional output (fusion). Moreover, the activated Ypt7 Rab itself opposes Yck3-mediated phosphorylation of Rab signaling targets. When the Rab is inactive, downstream functions are inhibited; when the Rab is active, it prevents inhibitory phosphorylation, and downstream functions are not inhibited. In the absence of the kinase, the Rab's downstream effectors are uninhibited, and even residual Rab signaling is sufficient to promote fusion.

Obviously, aspects of this working model are tentative. For example, the functional consequences of Yck3-dependent Vam3 phosphorylation are not yet characterized. However, Ungermann and colleagues have identified the site of Yck3-mediated phosphorylation within Vps41 and have confirmed that modification of this site inhibits Vps41 function (Ungermann, C., personal communication). At present, activated Ypt7-GTP is the only signal transducer known to regulate Yck3-dependent phosphorylation (Fig. 5). Ypt7-GTP could oppose Yck3-dependent phosphorylation by directly or indirectly inhibiting the intrinsic activity of Yck3 or by activating or localizing a phosphatase. Alternatively, Ypt7 could shield substrates from the Yck3 kinase through direct binding interactions, a possibility supported by our discovery that Vps41, a Yck3 target, also contains a Ypt7-binding site (Figs. 6 and 7).

Our data further suggest that a positive feedback loop controls activation of Ypt7 in a manner similar to that described for Rab5, its GEF Rabex-5, and its effector Rabaptin (Lippe et al., 2001). Vps39, the Ypt7 GEF (Wurmser et al., 2000), and Vps41 are physically associated as subunits of the Vps-C/HOPS tethering complex (Seals et al., 2000), and both subunits are necessary for specific binding of the HOPS holocomplex to Ypt7 in the presence of GTPγS (Fig. 6 c). Vps39-mediated activation of Ypt7 would generate additional binding sites for HOPS, thereby further stabilizing HOPS at the membrane and allowing Vps39 to engage in multiple cycles of Ypt7 activation (Fig. 7 b). Studies of Ypt7-regulated protein localization at vacuole-docking junctions provide additional support for the existence of a Vps39-mediated positive feedback loop (Wang et al., 2003). Because Vps41 is needed for stable HOPS binding to Ypt7, we predict that inactivation of Vps41 by Yck3 will terminate this positive feedback,

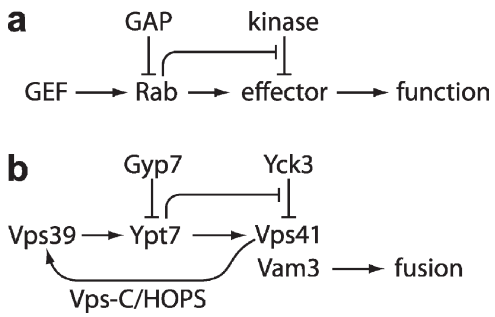


Figure 7. **Feed-forward inhibition of Ypt7 signaling.** (a) General scheme. (b) Implementation at the yeast vacuole. Lines terminating in arrows indicate positive regulation, and lines terminating in bars indicate inhibition. Vps39 and Vps41 are subunits of the Vps-C/HOPS protein complex, which also contains Vps11, 16, 18, and 33.

reducing the efficacy of Vps39-mediated Ypt7 activation. Experimental tests of these predictions are underway in our laboratory.

There are several examples of phosphorylation regulating Rab signaling pathways. The Rab GAP AS160 (Sano et al., 2003) regulates insulin-stimulated exocytosis of glucose transporters. When phosphorylated by Akt, AS160 is inhibited, permitting activation of its target, Rab10 (Roach et al., 2007; Sano et al., 2007). Phosphorylation also regulates downstream targets of Rabs, including SNARE proteins, in both yeast and mammals. For example, casein kinase II phosphorylates the synaptic $Q_a$-SNARE syntaxin 1A in vitro (Hirling and Scheller, 1996). Phosphorylation often inversely correlates with fusion. Yeast cells expressing a Golgi $Q_a$-SNARE Sed5 phosphomimetic mutant have fragmented Golgi compartments, whereas cells expressing a phosphorylation-resistant Sed5 mutant have ordered Golgi (Gurunathan et al., 2002; Weinberger et al., 2005). Rab effectors are also phosphorylated (Lonart and Sudhof, 1998; Lonart et al., 2003). For example, phosphorylation of the Rab11 effector Rip11 controls its localization on apical recycling endosomes within epithelial cells (Prekeris et al., 2000). Finally, the Ypt31/32 Rab GTPases regulate phosphorylation of the yeast R-SNARE Snc1 (Chen et al., 2005). Thus, interactions between Rab signaling and phosphorylation are pervasive.

A general problem in biological signal transduction is the maintenance of fidelity in circuits that, because they rely on small populations of molecules, operate in a noisy analogue mode. In these systems, negative feedbacks are used to maintain homeostatic equilibria, whereas positive feedbacks can amplify small signals or generate switchlike behaviors. We propose that the Ypt7 signaling pathway incorporates both a positive feedback loop that reinforces Ypt7 activation and a positive feed-forward loop (which uses two negative elements in series) that enforces the requirement for Ypt7 activation (Fig. 7). We propose that this circuit topology increases the fidelity of Ypt7-mediated signaling by suppressing spurious downstream signaling when an upstream signal falls below a specific threshold. This in turn renders the overall pathway more responsive to signals that impinge on Ypt7 by increasing the pathway's signal to noise ratio. Given the commonality of other strategies in small GTPase signaling (Grosshans et al., 2006; Bos et al., 2007), it is likely that such an arrangement will not be unique to the vacuolar Rab.

**Note added in proof.** We have identified conditions under which purified Vps41 binds selectively to Ypt7-GTPγS. To obtain homogenous Ypt7-GDP, GST-Ypt7 bound to ∼50 µl of glutathione-agarose beads is incubated with 5 µg $His_6$-$Gyp1_{TBC}$ overnight at 4°C and for 30 min at 23°C. The Gyp1 is removed. GST-Ypt7-GTPγS is prepared from GST-Ypt7-GDP by incubating the bead suspension for 90 min at 23°C in nucleotide exchange buffer (50 mM Tris-Cl, pH 8.0, 100 mM NaCl, 4 mM EDTA, and 5 mM 2-mercaptoethanol) containing 1.4 mM GTPγS. GTPγS loading is stopped by the addition of excess pull-down buffer (50 mM Tris-Cl, pH 8.0, 100 mM NaCl, 5 mM $MgCl_2$, and 5 mM 2-mercaptoethanol). The beads are washed twice in pull-down buffer, and Vps41 pull-down is performed as in Fig. 6 d.

# Materials and methods

### Strains and plasmids

For fusion assays, we used complimentary strain pairs of BJ3505 (*MAT*α *pep4*::*HIS3 prb1-1.6R his3-200 lys2-801 trp1-101* [*gal3*] *ura3-52 gal2 can1*) and DKY6281 (*MAT*α *leu2-3 leu2-112 ura3-52 his3-200 trp1-901 lys2-801*) or BY4742 *pep4*Δ (*MAT*α *ura3*Δ *leu2*Δ *his3*Δ *lys2*Δ *pep4*Δ::*neo* [Invitrogen]) and BY4742 *pho8*Δ::*neo*. BJ3505 *GFP-VPS39*, BJ3505 *gyp7*Δ::*URA3*, DKY6281 *gyp7*Δ::*URA3* or BJ3505 $YPT7_{Q68L}$::*neo*, and DKY6281 $YPT7_{Q68L}$::*neo* were provided by W. Wickner (Dartmouth College, Hanover, NH), G. Eitzen (University of Alberta, Edmonton, Canada), and D. Gallwitz (Max Planck Institute of Biophysical Chemistry, Göttingen, Germany). Double mutant *yck3*Δ *pep4*Δ (AMY807), *yck3*Δ *pho8*Δ (AMY809), *yck3*Δ *ypt7*Δ (AMY913), *yck3*Δ *vps41*Δ (AMY996), or *yck3*Δ *vps39*Δ (AMY999) cells were constructed by mating BY4741 (*MAT*α *ura3*Δ *leu2*Δ *his3*Δ *met15*Δ [Invitrogen]) with BY4742-derived haploid cells and sporulating; the genotypes of spores isolated by tetrad dissection were confirmed by mapping PCR. Gyp7-overproducing BY4742 wild-type, *gyp7*Δ, *ypt7*Δ, *yck3*Δ, *yck3*Δ*ypt7*Δ and BJ3505, DKY6281, or DKY6281 $YPT7_{Q68L}$ cells carried the plasmid pYADH1-*GYP7*-$His_6$ (*GYP7* with a C-terminal hexahistidine tag inserted behind the *ADH1* promoter in the 2-µ yeast shuttle vector [39967; American Type Culture Collection] D. Gallwitz). The set of regulated *GYP* plasmids was constructed by gap repair–mediated homologous recombination between the vector pCM190 (containing a tetracycline-repressible promotor; Gari et al., 1997), and each of the eight *GYP* genes or *GYL1* (a *GYP*-like gene) was amplified by PCR with primers containing terminal sequences homologous to pCM190. The resulting plasmids were rescued into *Escherichia coli*, amplified, sequenced, and transformed into *S. cerevisiae* BY4742. Transformants were selected in the presence of doxycycline and in the absence of uracil. Gyp overproduction was induced by removing doxycycline from the growth medium.

### Reagents

All biochemical reagents were purchased from Sigma-Aldrich or Invitrogen, except as indicated, and were of biotechnology grade or better. The endoglucanase fraction of Zymolyase (20T; Seikigaku) was purified by cation exchange chromatography before use in vacuole isolation. Calf intestinal phosphatase (CIP) was purchased from New England Biolabs, Inc. Purified proteins used include rGdi1 purified from bacterial cells using a calmodulin-binding peptide intein fusion system (provided by V. Starai, Dartmouth Medical School, Hanover, NH; and W. Wickner), $rGyp1_{TBC}$, recombinant soluble Qc-SNARE Vam7, and recombinant protease inhibitor Pbi2. Rabbit polyclonal sera raised against Vps41, Vps33, Ypt7, and Vam3 (provided by W. Wickner) were affinity purified and, in some cases, were cross-adsorbed against cell lysates from corresponding yeast deletion strains to reduce cross-reactivity. The protein reagents used in fusion assays were prepared in 10 mM Pipes-KOH, pH 6.8, and 200 mM sorbitol (Pipes-sorbitol buffer, PS) or were exchanged into this buffer by dialysis or size exclusion chromatography.

### Fusion

Vacuoles were purified as described previously by Haas et al. (1995). 6 µg of isolated vacuoles was incubated for 90 min at 27°C in standard reaction buffer as follows: PS buffer supplemented with salts (0.5 mM $MgCl_2$ and 125 mM KCl), 10 mM CoA, and Pbi2 with or without ATP-regenerating system (0.5 mM ATP, 0.1 mg/ml creatine kinase, and 40 mM creatine phosphate). Bypass fusion was initiated with 100 nM rVam7 in the presence of 1 mg/ml BSA. Osmotic gradients were imposed by reducing or adding sorbitol to the standard isotonic reaction buffer (200 mM sorbitol). As indicated, reactions also contained CIP, rGdi1, $rGyp1_{TBC}$, or GTPγS. The total volume of each fusion reaction was 30 µl. Fusion reactions were conducted using DKY6128 (or BY4742 *pho8*Δ; alkaline phosphatase deficient) and BJ3505 (or BY4742 *pep4*Δ; protease deficient) vacuoles (3 µg each) with or without genomic deletion of *GYP7* (*gyp7*Δ) or *YCK3* (*yck3*Δ), with *YPT7 or* $YPT7_{Q68L}$, or expression of pYADH1-*GYP7*-$His_6$ (+*GYP7*). Homotypic vacuole fusion was measured using a biochemical complementation assay (Haas et al., 1995; Merz and Wickner, 2004a). Fusion (content mixing) was quantified by monitoring the alkaline phosphatase–catalyzed evolution of *p*-nitrophenolate at 400 nm. Signals were then subtracted from a background control reaction either lacking ATP or incubated on ice; the signal to background ratio under our standard conditions routinely exceeds 25:1. Results are reported relative to signals obtained under standard fusion conditions (200 mM sorbitol with ATP or rVam7). Under standard conditions, the mean extent of fusion was 4.11 ± 0.12 ($n$ = 16) fusion units as previously defined (Haas et al., 1995; Merz and Wickner, 2004a). Vacuole membrane release or the phosphorylation state of Ypt7, Vam3, and HOPS components was determined using fusion reactions containing exclusively protease-deficient vacuoles (6 µg BJ3505 or BY4742 *pep4*Δ). After incubation at 27°C for 40 or 70 min, fusion reactions were immediately sedimented by centrifugation at 20,000 *g* for 5 min at 4°C. Pellet and supernatant fractions were separated by SDS-PAGE and analyzed by immunoblotting as indicated.

### Microscopy

To assess vacuole morphology in vivo, yeast were incubated for 1 h at 30°C in synthetic complete (SC) medium containing 3 µM FM4-64, sedimented, and resuspended in SC. After a 30-min chase period, cells were sedimented again, resuspended in either water, SC, or SC supplemented with 0.4 M NaCl, incubated for 5 or 30 min at 30°C, and imaged. To quantify cellular vacuole morphology phenotypes, at least six micrographs containing fields of ∼30 cells (from three independent cultures) were acquired, and cellular vacuole morphology was visually classified as either round or multilobed using the scheme of LaGrassa and Ungermann (2005; Fig. 1 b). Cells were scored as "round" if vacuoles were present as a single large or small spherical structure, a single large spherical structure with small adjoining vesicles, or two large oblong abutting structures. Cells were scored as "multilobed" (or fragmented) if they contained three or more small spherical structures or a single tubular structure with one or more spherical structures. All micrographs were acquired using a microscope (IX71; Olympus) equipped with an electron-multiplying charge-coupled device (iXon; Andor), ultrabright green and blue light-emitting diodes (>350-mW output) driven by custom electronics, a PlanApoN 1.45 NA 60× objective lens, and iQ software (version 6.0.3.62; Andor). Micrographs were processed using ImageJ (version 1.36b; National Institutes of Health) and Photoshop CS (version 8.0; Adobe) software. The images shown were adjusted for brightness and contrast and sharpened with an unsharp masking filter.

### Two-hybrid tests

Parent strains and plasmids were obtained from the University of Washington Yeast Resource Center. Two-hybrid plasmid constructs were constructed in haploid yeast strains by PCR-mediated homologous recombination cloning. ORF or domain sequences were amplified by PCR using primers containing terminal homology to the two-hybrid test vectors. Prey domains were cloned into gapped pOAD plasmid by cotransformation into the yeast strain PJ69-4 *MAT*α. Bait domains were cloned into pOBD2 in strain PJ69-4 *MAT*α. Clonal isolates were verified by PCR and DNA sequencing. Interaction tests were performed by mating bait and prey haploid strains. Liquid cultures of the bait and prey strains were grown in selective media, mixed in 96-well plates, and pinned to yeast extract–peptone–dextrose plates supplemented with adenine using a 48-spoke inoculating manifold. These mating plates were grown at 30°C overnight, and diploids were selected by replica plating onto medium lacking tryptophan and leucine and supplemented with adenine. Diploid colonies were grown at 30°C for 2 d, replica plated to medium lacking tryptophan, leucine, and histidine, and supplemented with adenine and 1.5 mM 3-amino-1,2,4-triazole. After 5 d at 30°C, the plates were scored for growth.

### GST-Rab pull-down assays

GST or GST-Rab fusion proteins were expressed in *E. coli* BL21-pRIL cells transformed with the vector pGST-Parallel-1 or with the same vector containing in-frame NcoI–BamHI PCR products encoding full-length Rab genes. Fusion proteins were coupled to glutathione–Sepharose 4B resin (GE Healthcare) as described previously for Ypt7 (Price et al., 2000), except coupling was performed in the absence of EDTA and EGTA, and 5 mM $MgCl_2$ was present throughout. Nucleotide loading of Rab proteins was performed by incubating Rab-bound resin in exchange buffer (50 mM Tris-HCl, pH 8.5, 100 mM NaCl, 0.01% 2-mercaptoethanol, 5 mM $MgCl_2$, and 500 µM guanine nucleotide) for 30 min. 50 µl of packed, nucleotide-loaded

GST-Rab resin was incubated with 500 µl of vacuole lysates, whole cell lysates, or recombinant Vps41 for 2 h. The resin was washed five times with 500 µl of lysis or solubilization buffer, and bound proteins and GST-Rabs were eluted by boiling reactions in 1× SDS buffer for 10 min. Equal loading of glutathione resins with Rab proteins was confirmed by SDS-PAGE. Whole cell lysates were similarly prepared as vacuoles, but after spheroplasting, cells were resuspended in lysis buffer (20 mM Hepes-KOH, pH 7.4, 50 mM potassium acetate, 200 mM sorbitol, 0.01% 2-mercaptoethanol, 5 mM $MgCl_2$, 0.7 µg/ml leupeptin, 0.5 µg/ml pepstatin, and 1 mM PMSF) and lysed by Dounce homogenization on ice. The lysate was solubilized with 1% Triton X-100 and clarified by centrifugation (20,000 *g* for 15 min). 500 µg of lysate protein was then added to the resin. Vacuole lysates were prepared by sedimenting 300 µg of isolated vacuoles (20,000 *g* for 10 min), resuspending membrane pellets in 500 µl of solubilization buffer (25 mM Hepes-KOH, pH 7.4, 125 mM NaCl, 10% glycerol, 0.5% Triton X-100, 5 mM $MgCl_2$, 0.01% 2-mercaptoethanol, and protease inhibitors), and clarifying soluble lysates by centrifugation (13,000 *g* for 10 min). Except as noted, all experiments were performed on ice or at 4°C.

### Preparation of recombinant Vps41

$His_6$-tagged Vps41 was expressed in Tn-5B1-4 (High-5) insect cells using the Bac-to-Bac system (Invitrogen). An in-frame BamH1–KpnI PCR product encoding full-length Vps41 was inserted into the shuttle vector pFB-HTB-N. The resulting plasmid was sequenced and transformed into DH10Bac *E. coli*, and bacmid DNA was purified from this strain. Bacmid DNA was transfected into Sf9 cells to prepare first, second, and third generation multiple nuclear polyhedrosis baculovirus stocks. Suspension-adapted High-5 cells were infected with virus, grown in suspension using SF-900 II serum-free media, supplemented with 100 U/ml penicillin, 10 µg/ml streptomycin, and 0.11 µg/ml L-glutamine for 72 h at 27°C, and harvested. Cell pellets were washed three times in PBS, resuspended in lysis buffer (50 mM Tris-HCl, pH 8.0, 350 mM NaCl, and 5 mM 2-mercaptoethanol), and lysed by sonication. Lysates were clarified by centrifugation (18,000 *g* for 20 min), incubated with pre-equilibrated nickel-nitrilotriacetic acid resin (GE Healthcare) for 1 h, and eluted using lysis buffer supplemented with 350 mM imidazole. The resulting eluate was size fractionated and exchanged into storage buffer (50 mM Tris-HCl, pH 8.0, 150 mM NaCl, 5 mM 2-mercaptoethanol, and 10% glycerol) on a Superdex 200 column (GE Healthcare). Aliquots of Vps41 were frozen in thin-walled PCR tubes by immersion in liquid nitrogen.

### Data analysis

Where applicable, datasets were fit to sigmoidal dose–response functions using a nonlinear least-squares algorithm. Log $IC_{50}$ values were extracted from the sigmoidal fits using Prism software (version 4.0c; GraphPad Software, Inc.). Data are reported as mean ± SEM. Mean comparisons were performed using Student's two-tailed *t* tests with corrections for multiple comparisons.

### Online supplemental material

Table S1 shows a summary of in vitro Rab specificities of the nine yeast Rab-GAP proteins. Fig. S1 shows that addition of GTP or GTPγS to vacuole fusion reactions overcomes inhibition of Ypt7 by rGdi1 or rGyp1TBC. Fig. S2 shows that deletion of *YCK3* is unable to suppress poor growth of *ypt7*Δ yeast at high temperatures. Fig. S3 shows a complete list of Vps41-interacting proteins obtained from our genome-wide yeast two-hybrid screen and control data validating the use of our two-hybrid miniarrays to evaluate Rab-binding selectivity. Online supplemental material is available at http://www.jcb.org/cgi/content/full/jcb.200801001/DC1.

We thank D. Gallwitz, G. Eitzen, and members of our group for critical discussions; W. Wickner, G. Eitzen, D. Gallwitz, and M. Kleijnen for generous gifts of antibodies and strains; and C. Ungermann for sharing unpublished results.

This work was supported by grant GM077349 from the National Institutes of Health. High throughput screening was performed by the National Center for Research Resources Yeast Resource Center which was supported by grant P41 RR11823 from the National Institutes of Health.

C.L. Brett and A.J. Merz conceived and designed the experiments. C.L. Brett performed most of the experiments. B.T. Lobinger prepared and characterized recombinant Vps41. R.L. Plemel constructed and analyzed yeast strains and performed two-hybrid miniarray analyses. M. Vignali and S. Fields designed and performed high throughput screening. C.L. Brett and A.J. Merz wrote the paper.

Submitted: 2 January 2008
Accepted: 19 August 2008

## References

Albert, S., E. Will, and D. Gallwitz. 1999. Identification of the catalytic domains and their functionally critical arginine residues of two yeast GTPase-activating proteins specific for Ypt/Rab transport GTPases. *EMBO J.* 18:5216–5225.

Ali, R., C.L. Brett, S. Mukherjee, and R. Rao. 2004. Inhibition of sodium/proton exchange by a Rab-GTPase-activating protein regulates endosomal traffic in yeast. *J. Biol. Chem.* 279:4498–4506.

Bone, N., J.B. Millar, T. Toda, and J. Armstrong. 1998. Regulated vacuole fusion and fission in *Schizosaccharomyces pombe*: an osmotic response dependent on MAP kinases. *Curr. Biol.* 8:135–144.

Bos, J.L., H. Rehmann, and A. Wittinghofer. 2007. GEFs and GAPs: critical elements in the control of small G proteins. *Cell.* 129:865–877.

Brett, C.L., and A.J. Merz. 2008. Osmotic regulation of Rab-mediated organelle docking. *Curr. Biol.* 18:1072–1077.

Chen, S.H., S. Chen, A.A. Tokarev, F. Liu, G. Jedd, and N. Segev. 2005. Ypt31/32 GTPases and their novel F-box effector protein Rcy1 regulate protein recycling. *Mol. Biol. Cell.* 16:178–192.

Collins, K.M., N.L. Thorngren, R.A. Fratti, and W.T. Wickner. 2005. Sec17p and HOPS, in distinct SNARE complexes, mediate SNARE complex disruption or assembly for fusion. *EMBO J.* 24:1775–1786.

Eitzen, G., E. Will, D. Gallwitz, A. Haas, and W. Wickner. 2000. Sequential action of two GTPases to promote vacuole docking and fusion. *EMBO J.* 19:6713–6720.

Gao, X.-D., S. Albert, S.E. Tcheperegine, C.G. Burd, D. Gallwitz, and E. Bi. 2003. The GAP activity of Msb3p and Msb4p for the Rab GTPase Sec4p is required for efficient exocytosis and actin organization. *J. Cell Biol.* 162:635–646.

Gari, E., L. Piedrafita, M. Aldea, and E. Herrero. 1997. A set of vectors with a tetracycline-regulatable promoter system for modulated gene expression in *Saccharomyces cerevisiae. Yeast.* 13:837–848.

Grosshans, B.L., D. Ortiz, and P. Novick. 2006. Rabs and their effectors: achieving specificity in membrane traffic. *Proc. Natl. Acad. Sci. USA.* 103:11821–11827.

Gurunathan, S., M. Marash, A. Weinberger, and J.E. Gerst. 2002. t-SNARE phosphorylation regulates endocytosis in yeast. *Mol. Biol. Cell.* 13:1594–1607.

Haas, A., D. Scheglmann, T. Lazar, D. Gallwitz, and W. Wickner. 1995. The GTPase Ypt7p of *Saccharomyces cerevisiae* is required on both partner vacuoles for the homotypic fusion step of vacuole inheritance. *EMBO J.* 14:5258–5270.

Hanson, P.I., R. Roth, H. Morisaki, R. Jahn, and J.E. Heuser. 1997. Structure and conformational changes in NSF and its membrane receptor complexes visualized by quick-freeze/deep-etch electron microscopy. *Cell.* 90:523–535.

Hirling, H., and R.H. Scheller. 1996. Phosphorylation of synaptic vesicle proteins: modulation of the alpha SNAP interaction with the core complex. *Proc. Natl. Acad. Sci. USA.* 93:11945–11949.

Jahn, R., T. Lang, and T.C. Sudhof. 2003. Membrane fusion. *Cell.* 112:519–533.

Kleijnen, M.F., D.S. Kirkpatrick, and S.P. Gygi. 2007. The ubiquitin-proteasone system regulates membrane fusion of yeast vacuoles. *EMBO J.* 26:275–287.

LaGrassa, T.J., and C. Ungermann. 2005. The vacuolar kinase Yck3 maintains organelle fragmentation by regulating the HOPS tethering complex. *J. Cell Biol.* 168:401–414.

Lippe, R., M. Miaczynska, V. Rybin, A. Runge, and M. Zerial. 2001. Functional synergy between Rab5 effector Rabaptin-5 and exchange factor Rabex-5 when physically associated in a complex. *Mol. Biol. Cell.* 12:2219–2228.

Lonart, G., and T.C. Sudhof. 1998. Region-specific phosphorylation of rabphilin in mossy fiber nerve terminals of the hippocampus. *J. Neurosci.* 18:634–640.

Lonart, G., S. Schoch, P.S. Kaeser, C.J. Larkin, T.C. Sudhof, and D.J. Linden. 2003. Phosphorylation of RIM1alpha by PKA triggers presynaptic long-term potentiation at cerebellar parallel fiber synapses. *Cell.* 115:49–60.

Mayer, A., W. Wickner, and A. Haas. 1996. Sec18p (NSF)-driven release of Sec17p (a-SNAP) can precede docking and fusion of yeast vacuoles. *Cell.* 85:83–94.

Merz, A.J., and W.T. Wickner. 2004a. Resolution of organelle docking and fusion kinetics in a cell-free assay. *Proc. Natl. Acad. Sci. USA.* 101:11548–11553.

Merz, A.J., and W.T. Wickner. 2004b. Trans-SNARE interactions elicit $Ca^{2+}$ efflux from the yeast vacuole lumen. *J. Cell Biol.* 164:195–206.

Milburn, M.V., L. Tong, A.M. deVos, A. Brunger, Z. Yamaizumi, S. Nishimura, and S.H. Kim. 1990. Molecular switch for signal transduction: structural differences between active and inactive forms of protooncogenic ras proteins. *Science.* 247:939–945.

Moya, M., D. Roberts, and P. Novick. 1993. DSS4-1 is a dominant suppressor of sec4-8 that encodes a nucleotide exchange protein that aids Sec4p function. *Nature.* 361:460–463.

Nichols, B.J., C. Ungermann, H.R. Pelham, W.T. Wickner, and A. Haas. 1997. Homotypic vacuolar fusion mediated by t- and v-SNAREs. *Nature.* 387:199–202.

Pan, X., S. Eathiraj, M. Munson, and D.G. Lambright. 2006. TBC-domain GAPs for Rab GTPases accelerate GTP hydrolysis by a dual-finger mechanism. *Nature.* 442:303–306.

Peplowska, K., D.F. Margraf, C.W. Ostrowicz, G. Bange, and C. Ungermann. 2007. The CORVET tethering complex interacts with the Yeast Rab5 homolog Vps21 and is involved in endo-lysosomal biogenesis. *Dev. Cell.* 12:739–750.

Pfeffer, S., and D. Aivazian. 2004. Targeting Rab GTPases to distinct membrane compartments. *Nat. Rev. Mol. Cell Biol.* 5:886–896.

Prekeris, R., J. Klumperman, and R.H. Scheller. 2000. A Rab11/Rip11 protein complex regulates apical membrane trafficking via recycling endosomes. *Mol. Cell.* 6:1437–1448.

Price, A., D. Seals, W. Wickner, and C. Ungermann. 2000. The docking stage of yeast vacuole fusion requires the transfer of proteins from a cis-SNARE complex to a Rab/Ypt protein. *J. Cell Biol.* 148:1231–1238.

Rehling, P., T. Darsow, D.J. Katzmann, and S.D. Emr. 1999. Formation of AP-3 transport intermediates requires Vps41 function. *Nat. Cell Biol.* 1:346–353.

Rieder, S.E., and S.D. Emr. 1997. A novel RING finger protein complex essential for a late step in protein transport to the yeast vacuole. *Mol. Biol. Cell.* 8:2307–2327.

Roach, W.G., J.A. Chavez, C.P. Miinea, and G.E. Lienhard. 2007. Substrate specificity and effect on GLUT4 translocation of the Rab GTPase-activating protein Tbc1d1. *Biochem. J.* 403:353–358.

Sano, H., S. Kane, E. Sano, C.P. Miinea, J.M. Asara, W.S. Lane, C.W. Garner, and G.E. Lienhard. 2003. Insulin-stimulated phosphorylation of a Rab GTPase-activating protein regulates GLUT4 translocation. *J. Biol. Chem.* 278:14599–14602.

Sano, H., L. Eguez, M.N. Teruel, M. Fukuda, T.D. Chuang, J.A. Chavez, G.E. Lienhard, and T.E. McGraw. 2007. Rab10, a target of the AS160 Rab GAP, is required for insulin-stimulated translocation of GLUT4 to the adipocyte plasma membrane. *Cell Metab.* 5:293–303.

Seals, D.F., G. Eitzen, N. Margolis, W.T. Wickner, and A. Price. 2000. A Ypt/Rab effector complex containing the Sec1 homolog Vps33p is required for homotypic vacuole fusion. *Proc. Natl. Acad. Sci. USA.* 97:9402–9407.

Segev, N. 2001. Ypt/rab gtpases: regulators of protein trafficking. *Sci. STKE.* doi: 10.1126/stke.2001.100.re11.

Sollner, T., M.K. Bennett, S.W. Whiteheart, R.H. Scheller, and J.E. Rothman. 1993. A protein assembly-disassembly pathway in vitro that may correspond to sequential steps of synaptic vesicle docking, activation, and fusion. *Cell.* 75:409–418.

Strom, M., P. Vollmer, T.J. Tan, and D. Gallwitz. 1993. A yeast GTPase-activating protein that interacts specifically with a member of the Ypt/Rab family. *Nature.* 361:736–739.

Thorngren, N., K.M. Collins, R.A. Fratti, W. Wickner, and A.J. Merz. 2004. A soluble SNARE drives rapid docking, bypassing ATP and Sec17/18p for vacuole fusion. *EMBO J.* 23:2765–2776.

Ungermann, C., B.J. Nichols, H.R. Pelham, and W. Wickner. 1998. A vacuolar v-t-SNARE complex, the predominant form in vivo and on isolated vacuoles, is disassembled and activated for docking and fusion. *J. Cell Biol.* 140:61–69.

Vollmer, P., E. Will, D. Scheglmann, M. Strom, and D. Gallwitz. 1999. Primary structure and biochemical characterization of yeast GTPase-activating proteins with substrate preference for the transport GTPase Ypt7p. *Eur. J. Biochem.* 260:284–290.

Wang, L., E.S. Seeley, W. Wickner, and A.J. Merz. 2002. Vacuole fusion at a ring of vertex docking sites leaves membrane fragments within the organelle. *Cell.* 108:357–369.

Wang, L., A.J. Merz, K.M. Collins, and W.T. Wickner. 2003. Hierarchy of protein assembly at the vertex ring domain for yeast vacuole docking and fusion. *J. Cell Biol.* 160:365–374.

Wang, Y.X., N.L. Catlett, and L.S. Weisman. 1998. Vac8p, a vacuolar protein with armadillo repeats, functions in both vacuole inheritance and protein targeting from the cytoplasm to vacuole. *J. Cell Biol.* 140:1063–1074.

Weber, T., B.V. Zemelman, J.A. McNew, B. Westermann, M. Gmachl, F. Parlati, T.H. Sollner, and J.E. Rothman. 1998. SNAREpins: minimal machinery for membrane fusion. *Cell.* 92:759–772.

Weinberger, A., F. Kamena, R. Kama, A. Spang, and J.E. Gerst. 2005. Control of Golgi morphology and function by Sed5 t-SNARE phosphorylation. *Mol. Biol. Cell.* 16:4918–4930.

Wichmann, H., L. Hengst, and D. Gallwitz. 1992. Endocytosis in yeast: evidence for the involvement of a small GTP-binding protein (Ypt7p). *Cell.* 71:1131–1142.

Wickner, W., and A. Haas. 2000. Yeast homotypic vacuole fusion: a window on organelle trafficking mechanisms. *Annu. Rev. Biochem.* 69:247–275.

Wurmser, A.E., T.K. Sato, and S.D. Emr. 2000. New component of the vacuolar class C-Vps complex couples nucleotide exchange on the Ypt7 GTPase to SNARE-dependent docking and fusion. *J. Cell Biol.* 151:551–562.

Zerial, M., and H. McBride. 2001. Rab proteins as membrane organizers. *Nat. Rev. Mol. Cell Biol.* 2:107–117.

Zhang, X.M., B. Walsh, C.A. Mitchell, and T. Rowe. 2005. TBC domain family, member 15 is a novel mammalian Rab GTPase-activating protein with substrate preference for Rab7. *Biochem. Biophys. Res. Commun.* 335:154–161.